

Eigenmode Expansion Methods for Simulation of Optical Propagation in Photonics - Pros and Cons

Dominic F.G. Gallagher, Thomas P. Felici
 Photon Design, Oxford,
 United Kingdom, www.photond.com

Keywords: Software, CAD, waveguide, photonics, modelling, eigenmode, EME, BPM.

ABSTRACT

With the rapid growth of the telecommunications industry over the last 5 to 10 years has come the need to solve ever more complex electromagnetic problems and to solve them more precisely than ever before. The basic EME (EigenMode Expansion) technique is a powerful method for calculation of electromagnetic propagation which has been well known amongst academic environments and also in microwave fields, representing the electromagnetic fields everywhere in terms of a basis set of local modes. It is at the same time a rigorous solution of Maxwell's Equations and is able to deal with very long structures. We discuss here progress that the authors and others have made recently in applying and extending it to integrated, fibre, and diffractive optics – including development of efficient ways of modelling tapers and other smoothly varying structures, new more efficient boundary conditions and improved mode finders. We outline the advantages it has over other techniques and also its limitations. We illustrate its application with a variety of real life examples, including diffractive elements, directional couplers, tapers, MMI's, bend modelling, periodic structures and others.

1. INTRODUCTION

In this paper we shall begin by explaining the fundamental theory of the EME (EigenMode Expansion) technique; then proceed with a more detailed description of the application of the basic theory to different computational elements. We shall illustrate the technique by reference to our implementation of EME – the program FIMMPROP. In the last section of this paper we shall present a number of FIMMPROP simulations to provide concrete numbers for the speed and efficiency of the method.

2. OUTLINE OF THE EME METHOD

The EME technique has been well established in photonics for some time^{1, 2}. It is a very simple technique in essence. We must start with a definition of the “mode” or “eigenmode” of a waveguide. In a structure where the *optical refractive index does not vary in the z direction*, we find solutions of Maxwell's Equations of the form

$$\underline{E}(x, y, z) = \underline{e}_m(x, y) \cdot e^{i\beta_m z}$$

(we assume here a single wavelength and time dependence of the form $\exp(i\omega t)$)

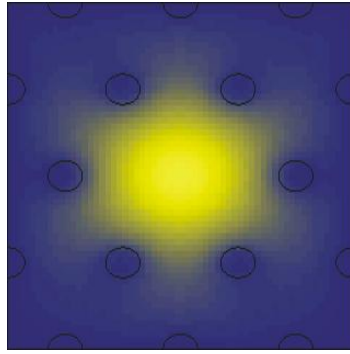


Figure 1: mode of a holey fibre

Mathematically $e_m(x,y)$ and β_m are the eigenfunction and eigenvalue of the solution. So a mode has a very simple harmonic z-dependence – this simple z-dependence is the key to enabling EME to solve long slowly varying structures quickly and efficiently – as we shall see later.

In a typical waveguide, there are a few *guided modes* (which propagate without loss along the waveguide), but in addition there are an infinite number of *radiation modes* (which carry optical power away from the waveguide).

The guided and radiation modes together form a *complete basis set* – in other words we can express *any solution* of Maxwell's Equations in the region of the waveguide in terms of a superposition of the forward and backward propagating modes (see Eqn 2):

$$\begin{aligned} \mathbf{E}(x, y, z) &= \sum_{k=1}^M (a_k e^{i\beta_k z} + b_k e^{-i\beta_k z}) \mathbf{E}_k(x, y) && \text{electric field} \\ \mathbf{H}(x, y, z) &= \sum_{k=1}^M (a_k e^{i\beta_k z} - b_k e^{-i\beta_k z}) \mathbf{H}_k(x, y) && \text{magnetic field} \end{aligned}$$

propagation constant
forward amplitude backward amplitude mode profiles

Notice the bi-directional nature of this equation. This equation is an *exact* solution of Maxwell's Equations in a linear medium.

So far we have a technique for analysing only z-invariant structures. Next we introduce a join between two waveguides – see Figure 2.

Maxwell's Equations gives us continuity conditions for the fields, e.g. the tangential electric fields must be equal on each side of the interface:

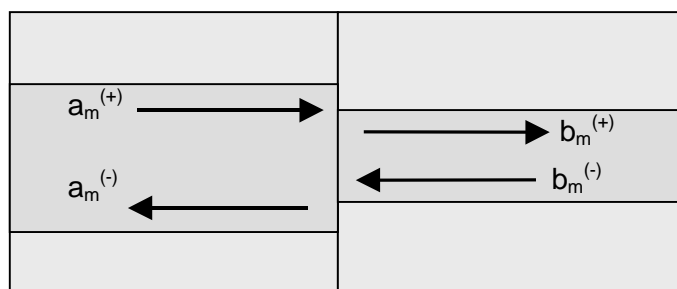


Figure 2: mode coefficients at a join

$$\sum_{k=1}^N \left(a_k^{(+)} e^{i\beta_k z} - a_k^{(-)} e^{-i\beta_k z} \right) \mathbf{E}_{k,t}^{(a)}(x,y) = \sum_{k=1}^N \left(b_k^{(+)} e^{i\beta_k z} - b_k^{(-)} e^{-i\beta_k z} \right) \mathbf{E}_{k,t}^{(b)}(x,y)$$

Applying these conditions, also conditions on the longitudinal electric field and the fields, and noting that the modes are orthonormal:

$$\int (E_{x,j} \cdot H_{y,k} - E_{y,j} \cdot H_{x,k}) \cdot d\underline{S} = \delta_{jk}$$

then after a little mathematics we can deduce a relationship between the coefficients of the form:

$$\begin{pmatrix} \underline{a}^{(-)} \\ \underline{b}^{(+)} \end{pmatrix} = S_J \begin{pmatrix} \underline{a}^{(+)} \\ \underline{b}^{(-)} \end{pmatrix}$$

where S_J is a *scattering matrix* for the join. So we have expressed the fields *travelling away* from the join in terms of the fields *incident on* the join. The scattering matrix S_{WG} for a straight section is simply:

$$\begin{pmatrix} e^{i\beta_1 z} & 0 & 0 & \dots \\ 0 & e^{i\beta_2 z} & 0 & \dots \\ 0 & 0 & e^{i\beta_3 z} & \dots \\ \vdots & \vdots & \vdots & \ddots \end{pmatrix}$$

which is clearly trivial to compute once the eigenmodes have been found. Let us now consider a common component used in photonics – the MMI coupler – see Fig. 3.

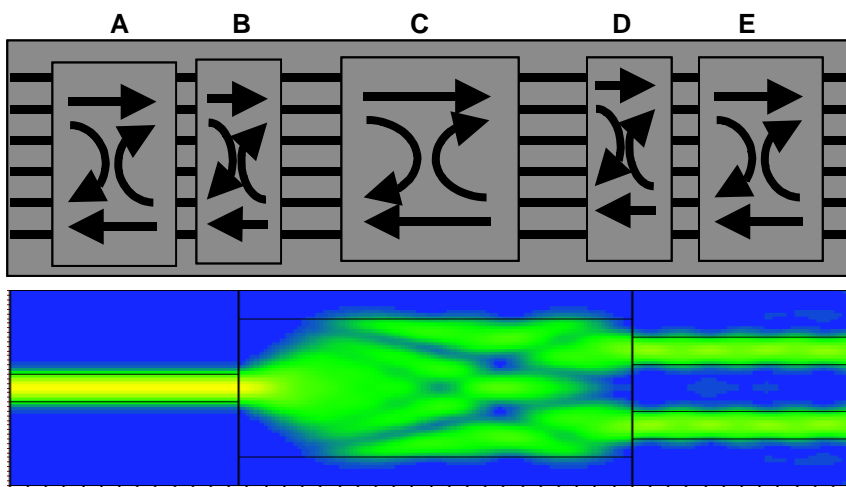


Figure 3: S-matrix decomposition of an MMI coupler

The device is described by 5 S-matrices – 2 join matrices and 3 propagation matrices. Once we have these individual S-matrices, we can compute combined S-matrices, e.g. the matrix AB by combining A and B, until we obtain an S-matrix for the whole device.

2.1 SMOOTHLY VARYING GEOMETRIES

One of the main reasons that EME was thought inappropriate in the early days was because of the difficulty of dealing efficiently with structures of continually changing cross-section, such as a taper. When the cross-section changes, all the modes need to be re-computed and this takes a lot of computational effort. Also one must introduce a large number of joins – which causes numerical errors to build up. FIMMPROP – our implementation of EME – contains features to solve both of these problems, enabling EME to be used realistically for the first time even for 3 dimensional tapering structures. In fact, instead of being slower than alternative approximate techniques, FIMMPROP can often solve a 3D taper structure in less time than the approximate techniques. Once having solved these problems, EME provides a very powerful tool for modelling near adiabatic structures – for the simple reason that near-adiabaticity is essentially a modal phenomenon – EME directly calculates the mode resonances, mode coupling and beating occurring in such devices, giving very valuable information to the designer for the improvement of his/her structures.

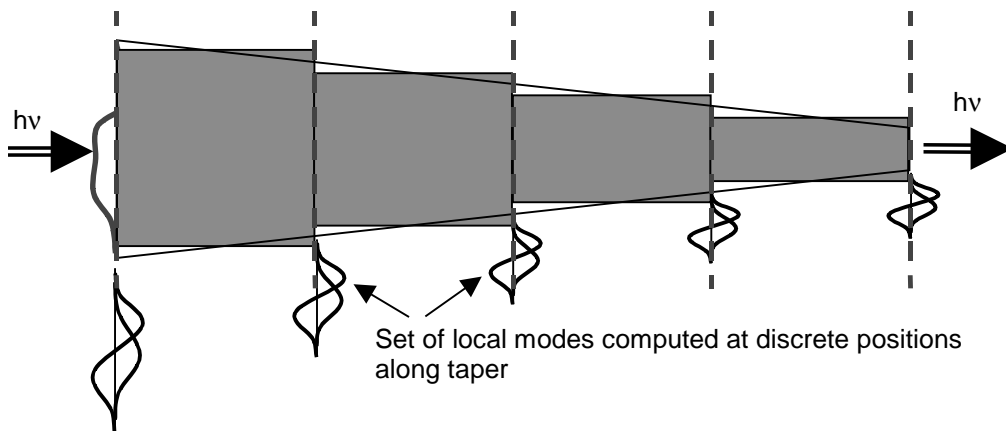


Figure 4: staircase approximation of a taper (zero-order integration)

A slowly varying structure may be modelled using a staircase approximation (zero-order case) or using a first- order integration. Figure 4 illustrates the zero order approximation – local modes are computed at discrete positions along the taper. This technique has the disadvantage of introducing non-physical reflections at the section interfaces which can give rise to significant spurious resonances for long structures. In theory this is exact as the number of sections tends to infinity but as well as the computational load associated with using many sections, there is a finite error with each section which accumulates. To avoid these problems we need to go to the first order approximation illustrated in figure 5.

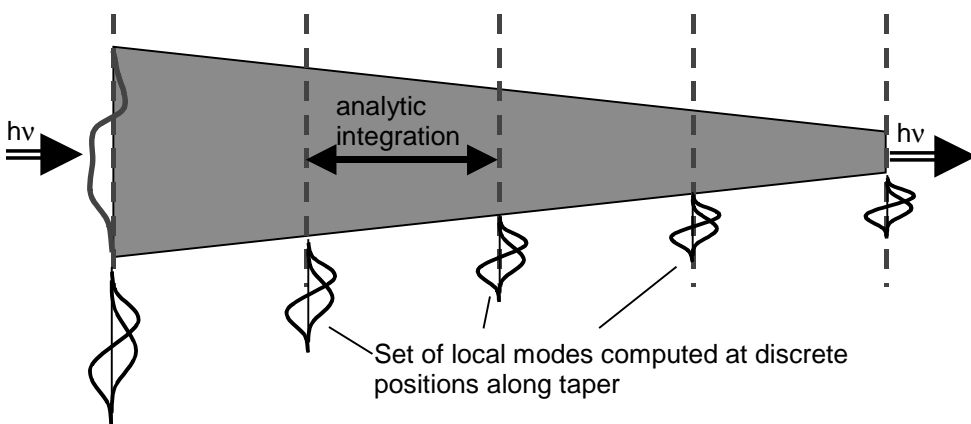


Figure 5: first-order integration of a taper improves computational efficiency

2.2 PERIODIC STRUCTURES

A structure composed of repeating identical periods can be computed efficiently using EME since the S-matrix of one period will be the same as that of every other period. Thus periodic structures can be computed almost as quickly as a straight waveguide.

2.3 BENDS

In an EME framework, a bend may be thought of as a set of straight waveguides with small tilts between each section. The modes of the straight waveguides may be readily found and the tilting of the phase front at the end of the section is trivial to compute. Notice that we have a periodic structure here – if the radius of curvature is constant, then each section of the bend is similar to the previous one. This is illustrated schematically in Figure 6 (left) below. On the right is an s-bend computed with such an algorithm (the bend has been straightened out for plotting purposes).

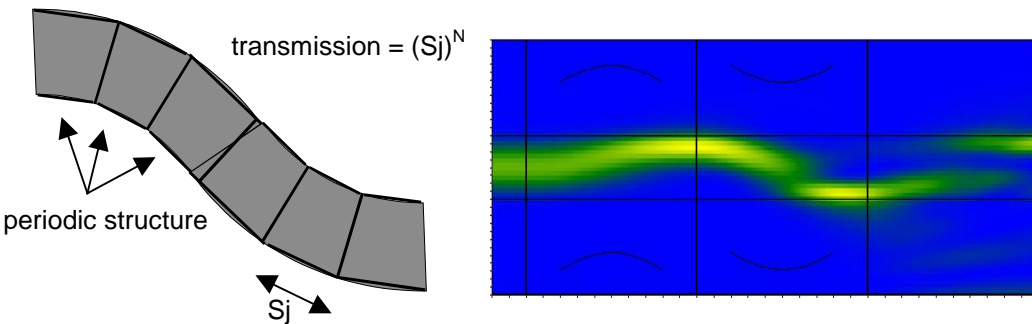


Figure 6 (left) EME computes a bend using a periodic algorithm, from many short straight waveguides. (right) simulation of an S-bend showing light veering towards the outside of the bend.

2.4 BOUNDARY CONDITIONS

The boundary conditions available with EME depends principally on the method used to locate the eigenmodes of the basis set. One or more of the following may be available:

- PEC and PMC – perfect electric/magnetic conductors. These are particularly useful for exploiting symmetries.
- Transparent boundary conditions
- PML's – perfect matched layers

Transparent boundary conditions are naturally imposed on the input and exit faces of the EME computation. Finding eigenmodes with true transparent boundary conditions generally leads to *leaky modes* and these can cause problems in obtaining a complete basis set. The PML³ is better suited to EME since it readily produces a more complete basis set. The PML is an additional layer with a complex thickness – see Figure 7. The imaginary part of this thickness is able to cause an absorption or decay in any fields propagating toward the boundary. And if the refractive index of the PML is kept similar to the cladding index then no reflection is imposed at the boundary of the PML – so we get as much absorption as we wish without parasitic reflections! So what does an imaginary thickness mean? Originally the imaginary coordinate was introduced in an ad-hoc way to obtain the desired properties, but Sacks⁴ showed that this is equivalent to an anisotropic material with a peculiar refractive index tensor.

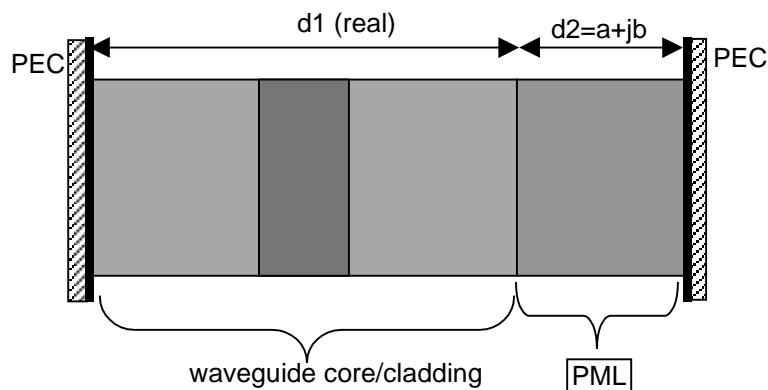


Figure 7: PML with imaginary thickness

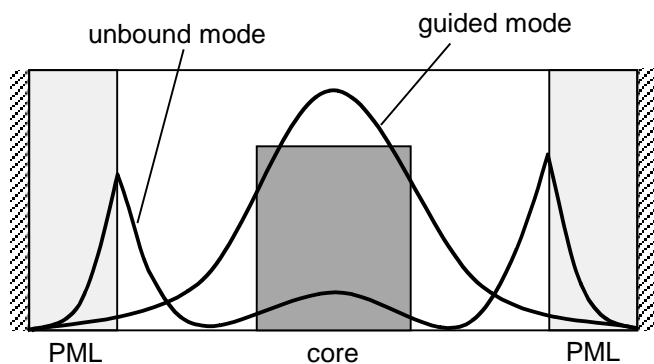


Figure 8: showing absorption of unbound modes by PML

3. WHY USE EME?

So why would you want to use EME? Although the reader might consider the authors to be somewhat biased (with some justification!), we will try to provide an objective assessment of the strengths and weaknesses of the method.

3.1 PROS AND CONS

Advantages:

- Firstly and most importantly the method is based on a rigorous solution of Maxwell's Equations. In principle we can obtain an exact solution if we use an infinite number of modes in our expansion. Of course in practice, we must limit the number used and there will be numerical errors in the implementation, as in any numerical technique. To obtain higher accuracy we can simply add more modes. This enables the method to accurately compute problems that are not possible with other techniques.
- The algorithm is inherently bi-directional. All reflections are taken into account in the method.
- The S-matrix technique provides the solution *for all inputs!* So for example if you do a fully vectorial simulation, you will get the response for both a TE and a TM input in the one calculation.
- The previous quality permits one to build up a component-like framework where the S-matrix of one component may be computed once and then re-used in many different contexts.
- When one part of a device is altered only the S-matrix of that part needs to be re-computed. So in Figure 3, if the alignment of the input waveguide were altered, only matrix B would need re-computing. FIMMPROP takes full advantage of such opportunities. In fact the program does not need a "calculate" button since it always knows what has changed and what needs re-computing at any time.

- Wide-angle capability – the method can simulate light propagating at any angle, even 90 degrees to the propagation axis, simply by adding more modes.
- The optical resolution and the structure resolution may be different.

The combination of the above properties permits a wide class of devices to be computed exceedingly quickly compared to other techniques. In general, structures with relatively small cross-section can be computed much more quickly than by other techniques – typically seconds instead of minutes or minutes instead of hours.

Disadvantages:

- Structures with very large cross-section are less suitable for the method since computational time typically scales in a cubic fashion with e.g. cross-section width.
- The algorithms are much more complex to write - for example it is very difficult to ensure that a mode has not been missed from the basis set.
- EME is not a “black box” technique – the operator must make some effort to understand the method to use it to his best advantage.

3.2 COMPUTATION TIME

It is useful to compare the computational efficiency of EME with the other two methods widely used in photonics CAD – FD-BPM and FDTD. We will restrict the discussion to 2D simulations – i.e. z and one lateral dimension. Both BPM and FDTD require a finite difference gridding of the structure so that the structure is sampled at these grid points. This same grid is used to resolve the optical field. In contrast, EME does not need a grid on the structure – uniform rectangular regions may be treated analytically. The equivalent of the optical grid in BPM and FDTD is the number of modes in the EME basis set – the more modes, the higher the spatial resolution that the basis set can resolve.

For a straight or nearly straight waveguide (near-adiabatic limit) the EME method is particularly efficient – it can propagate along 1m of waveguide as easily as 1um. In contrast the finite difference methods must discretise even near-uniform structures. For a periodic structure, BPM and FDTD must propagate through each period one after the other. In contrast, EME can find the scattering matrix of one period and then all other periods are the same – producing a logarithmic dependence with the number of periods. However where the structure has an arbitrary z-dependence, then all 3 methods have a similar linear dependence with z-complexity/resolution.

In the lateral dimension, EME can obtain very high spatial resolution for nominal cost – the modes of a 10 layer structure can be found almost as easily as the modes of a 2 layer structure, and for 2D simulations at least, mode finding takes a nominal time. In contrast, it is expensive in BPM to increase the structural resolution – even if there is just one small feature such as a thin layer to capture, BPM does not like non-uniform grids (for stability reasons) so that a fine grid must be applied everywhere. On the other hand, the computational load for lateral optical resolution is high for EME – since this resolution is determined by the size of the basis set (number of transverse modes used in the expansion). The size of the scattering matrices is the size of the basis set and all but the most trivial of matrix operations are cubic in computation load. This cubic factor is *the* major limit on the application of EME.

These factors are summarized in Table 1 below.

Table 1: Computation time – dependence on spatial resolution (2D simulation)

	BPM	FDTD	EME
Straight waveguide – z dependence	N^1	N^1	N^0
Near adiabatic structure – e.g. taper	N^1	N^1	$N^0 \rightarrow N^1$
Periodic structure – z dependence	N^1	N^1	$\log(N)$
Generic structure – z dependence	N^1	N^1	N^1
Cross-section – structural resolution	N^1	N^1	$\epsilon \cdot N^1$, ϵ small
Cross-section – optical resolution	N^1	N^1	N^3

3.3 MEMORY REQUIREMENTS

For similar reasons to those discussed above, EME is very efficient in memory usage as a function of z resolution. For a straight waveguide one set of modes may model a length of 1um or 1m. So it can obtain a N^0 scaling with z-resolution. For obvious reasons, if one wants the field profiles too then this becomes N^1 . Uni-directional BPM can in principle throw away the field profiles as it propagates – thus also achieving an N^0 dependence. FDTD needs to store field profiles everywhere at each time step (to obtain the wavelength dependence later) and in general, the larger the structure, the more time steps are needed – thus we get an N^2 dependence in each dimension. For this reason, FDTD is a very memory intensive technique.

In the lateral dimension, higher optical resolution requires more modes, and if the field profiles are needed then each mode must be evaluated at more points – thus EME has an N^1 dependence with lateral size/resolution if just the scattering matrices are required and an N^2 dependence if the field profiles are required too.

These factors are summarized in Table 2 below.

<i>Table 2: Memory requirements – dependence on spatial resolution (2D simulation)</i>			
	BPM	FDTD	EME
Straight waveguide – z dependence	$N^0 \rightarrow N^1$	$N^1 \rightarrow N^2$	$N^0 \rightarrow N^1$
Periodic structure – z dependence	$N^0 \rightarrow N^1$	$N^1 \rightarrow N^2$	$N^0 \rightarrow N^1$
Generic structure – z dependence	$N^0 \rightarrow N^1$	$N^1 \rightarrow N^2$	N^1
Cross-section – structural resolution	N^1	$N^1 \rightarrow N^2$	N^0
Cross-section – optical resolution	N^1	$N^1 \rightarrow N^2$	$N^1 \rightarrow N^2$

4. APPLICATIONS

It is useful to illustrate the features of EME by reference to a few concrete examples. Where we give computation times, these have been obtained running FIMMPROP on a 1GHz Pentium III.

4.1 THE MMI COUPLER

Figure 3 above shows an MMI coupler, and the optical intensity distribution as computed by FIMMPROP. This is a trivial application for EME – we need to compute only 3 sets of modes, one set for each unique cross-section.

Computation type:	semi-vector, 3D, bi-directional
Cross-section:	20 μm x 2.6 μm .
Number of modes:	8
Computation Time:	27s

In Figure 9 we plot the result of a design curve scan. The program has varied the offset of the input waveguide from 0 μm to 3 μm in 50 steps. To do all 50 simulations took just 94s, under 2s per simulation – remember this is a fully 3D computation!

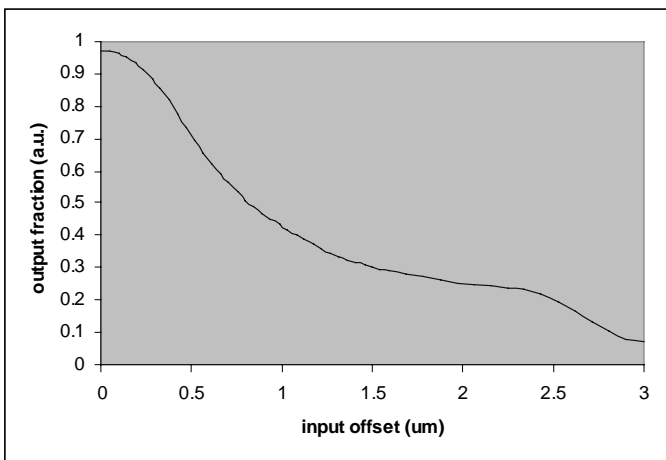


Figure 9: MMI efficiency as a function of input waveguide alignment.

4.2 A TAPERED FIBRE

Here we compute the propagation of light through a fibre tapering down from a core radius of $12\mu\text{m}$ to a radius of $0.5\mu\text{m}$. The computation details are shown below.

Computation type:	full-vector, 3D, bi-directional
Cross-section:	$38\mu\text{m} \times 38\mu\text{m}$
Number of modes:	6
Computation Time:	159s

The result of the computation is shown in Figure 10. Note how few modes we needed for this simulation – just 6. This is because most of the light is travelling at only small angles to the z-axis. One of the key questions that a designer will need to know about such a taper is “how long should it be to attain (e.g) 98% efficiency?” The EME technique can answer this question very quickly – altering the length of the taper does not alter the modes so that we can do many lengths for minimal additional computation time. Figure 11 plots the result of a length scan on the taper using 50 steps. The 50 simulations took 323s to compute – or just 6.5s per simulation.

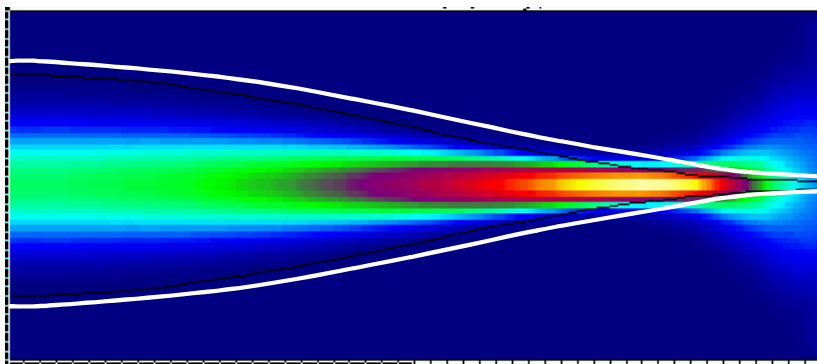


Figure 10: optical intensity along a fibre taper – computed by EME

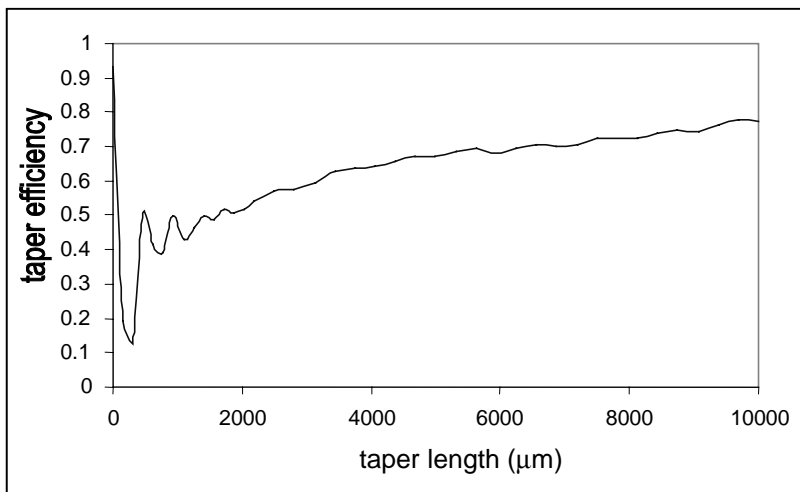


Figure 11: variation of taper efficiency with device length

A particularly valuable feature of EME is that it often gives one a detailed physical picture of what is going on in a device – rather than simply showing what comes in and what goes out, it can often tell one why something is occurring and so how to control the occurrence. It is well known that in a near adiabatic structure, coupling between modes occurs strongest when they have very similar propagation constants. Figure 12 shows the effective indices of the modes of this taper as a function of z-position for a 100um long device. The figure shows us immediately that the fundamental mode becomes very close to the higher order mode at 90% of taper length (90um). Thus we would expect most radiation at this point – and indeed this is exactly what we observe. The curve tells us that if possible, we should reduce the taper speed towards the end of the taper.

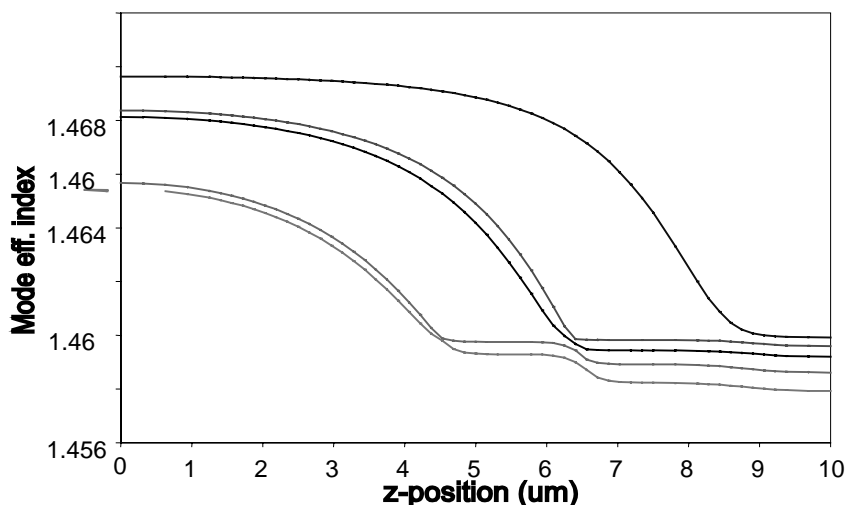


Figure 12 effective indices of the first 5 modes of a fibre taper. Strong coupling occurs when the effective indices are close – telling us where the trouble spots of the device are.

4.3 A CO-DIRECTIONAL COUPLER

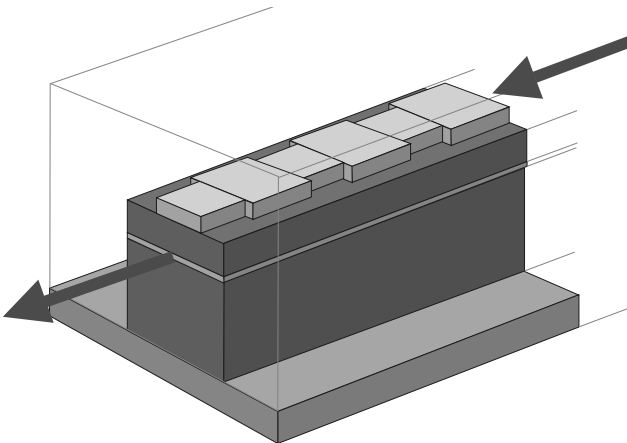


Figure 13: a co-directional coupler, coherently coupling light in upper guide to the thin lower layer

The scattering matrix basis of the EME technique is ideal for periodic structures, allowing speed acceleration by factors of 10, 100 or more. The method calculates the S-matrix of one period and then re-uses this S-matrix for every period – the result is a calculation time that is logarithmic with the number of periods. Figure 13 above illustrates a typical periodic device modelled by us with EME as part of the European COST240 project. The device is designed to couple light from the top waveguide to the fundamental mode of the thin layer underneath. This structure has been proposed as a convenient beam expander.

4.4 A RING RESONATOR

An illustration of the power and flexibility of EME is its ability to simulate wide angle and even omni-directional problems as efficiently as near paraxial ones. Figure 14 shows the fields computed by FIMMPROP in a double ring resonator. Computational details are given in the table below for a single ring.

Computation type:	Full-vector, 2D, bi-directional
Computational window:	6 μm x 6 μm
Number of modes:	60 (for one ring)
Computation Time: (S-matrix)	58s (for one ring)

Note that for such a wide angle calculation, we require many more modes.

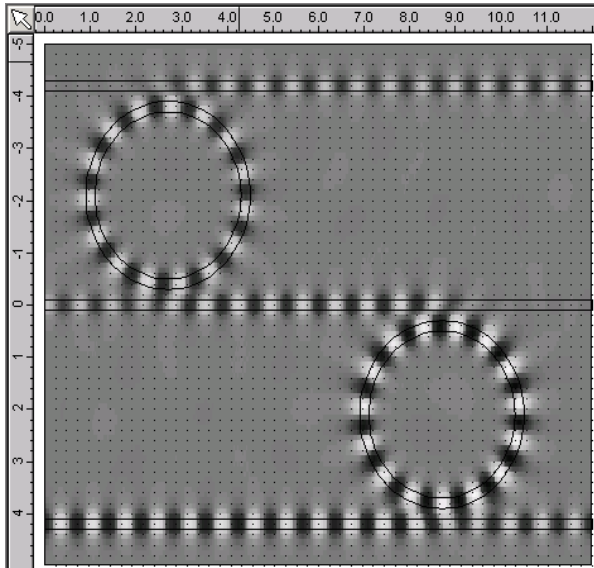
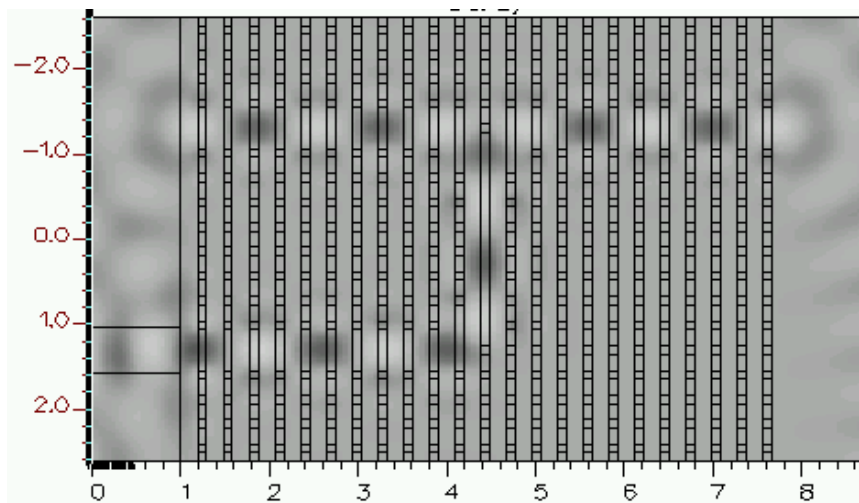


Figure 14: Ey field distribution computed in ring resonator structure.

The BPM technique, because of its paraxial approximation is fundamentally incapable of simulating such a structure and the alternative to EME here is the FDTD technique. FDTD has its own strengths and weaknesses. For a resonant structure such as this, the time domain nature of the FDTD method means that it takes a long time to settle down to a precise steady state. In contrast, the frequency domain EME method delivers a precise wavelength response without iteration.

4.5 PHOTONIC CRYSTAL DESIGN

The new subject of photonic crystals has presented a range of new challenges to photonic simulation techniques. EME is capable of simulating 2D photonic crystal lattice structures in an efficient manner. The S-matrix nature of EME is able to take advantage of much of the repetition in a photonic crystal so that computation time is usually sub-linear with device length. Figure 15 below shows the result of the simulation of a T-junction in a 2D lattice.



I **Figure 15:** Ey field through a T-junction in a photonic crystal lattice.

The table below shows some computation results – just 19s. Here we have used square holes – a more realistic approximation of round holes would double or triple the computation time.

Computation type:	Full-vector, 2D, bi-directional
Computational window:	5μm x 9μm
Number of modes:	60
Computation Time: (S-matrix)	19s

4.6 VCSEL MODELLING

EME has been extensively and very successfully used for the modelling of VCSEL cavities. Indeed it is a very efficient tool for this application. VCSELs generally have a cylindrical symmetry which means that they can be readily modelled using a Bessel Function basis set. Whereas the propagation problems described previously simulated the response of a device to an optical source placed outside the device and of known wavelength, to model a VCSEL we require:

- a) determination of the threshold gain – the lasing mode requires a gain to exactly equal the losses of the cavity.
- b) determination of the resonant wavelength – the VCSEL will only resonate at particular, discrete wavelengths. In other words we have to find an eigenvalue of the 3 dimensional cavity

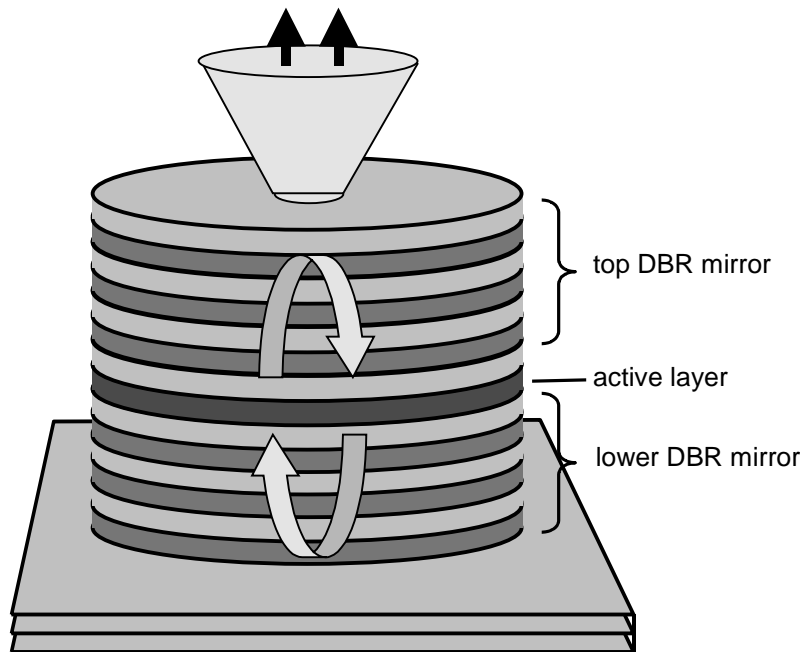


Figure 16: Schematic of a VCSEL – readily modelled by EME using a Bessel Function basis set

The cavity mode must obey the resonance condition

$$\underline{R}_{top} \cdot \underline{R}_{bot} \underline{u} = g \underline{u}$$

See figure 17. The \mathbf{R} are the *scattering matrices* for reflection from top and bottom stacks, \mathbf{u} is the *eigenvector* of coefficients of the transverse modes and \mathbf{g} is the **eigenvalue** of the system. To obtain lasing \mathbf{g} must be unity – to achieve this both the gain of the active layer and the wavelength must be determined.

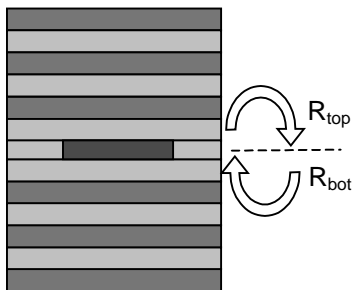


Figure 17: resonance condition of VCSEL

5. CONCLUSIONS

We have presented the basis of the EME technique for the rigorous modelling of optical propagation, and its pros and cons relative to its computational competitors. This powerful method is able to adapt efficiently to a wide variety of calculations from the near paraxial case of a nearly adiabatic structure such as a tapered fibre to the omni-directional case of propagation in a ring resonator or photonic crystal. It is a naturally bi-directional, taking into account all reflections. It has very substantial speed advantages over other methods for many categories of device including long tapers, periodic structures and photonic crystals. The ready availability of all the cross-section modes and their propagation constants also provides important insights into the functioning of a photonic component that helps the designer both to understand the physical mechanisms occurring and also provides important hints on how to improve the component.

¹ Peng, S.-T. and A. A. Oliner. *Guidance and leakage properties of a class of open dielectric waveguides: Part I mathematical formulations*. IEEE-MTT **29**, pp. 843-855, 1981.

² Sudbo, A. S., *Film mode matching: a versatile numerical method for vector mode field calculations in dielectric waveguides*. Pure Appl. Opt. **2**, pp. 211-233, 1993.

³ J.P. Berenger, *A perfectly matched layer for the absorption of electromagnetic radiation*, J. Compt. Phys. **114**, pp. 185-200, 1994.

⁴ Z. Sacks, D. Kingsland, R. Lee, J. Lee, *A perfectly matched anisotropic absorber for use as an absorbing boundary condition*, IEEE Trans. Antennas Propagat. **43**, pp. 1460-1463, 1995.